

Systems with disorder, interactions, and out of equilibrium: The exact independent-particle picture from density functional theory

Daniel Karlsson,¹ Miroslav Hopjan,^{2,3} and Claudio Verdozzi^{2,3}

¹Department of Physics, Nanoscience Center P.O.Box 35 FI-40014 University of Jyväskylä, Finland*

²Department of Physics, Division of Mathematical Physics, Lund University, 22100 Lund, Sweden

³European Theoretical Spectroscopy Facility, ETSF

Density functional theory (DFT) exploits an independent-particle-system construction to replicate the densities and current of an interacting system. This construction is used here to access the exact effective potential and bias of non-equilibrium systems with disorder and interactions. Our results show that interactions smoothen the effective disorder landscape, but do not necessarily increase the current, due to the competition of disorder screening and effective bias. This puts forward DFT as a diagnostic tool to understand disorder screening in a wide class of interacting disordered systems.

PACS numbers: 71.27.+a, 72.10.Bg, 71.23.An

How disorder and electron correlations shape material properties is a major question of current condensed matter research [1]. The interest in this problem is many decades old [2–8], and significant progress has been made in important directions, e.g. in describing the correlation-induced Mott-Hubbard [9] and the disorder-induced Anderson [10] metal-insulator transition. Yet, a complete general understanding of the joint effect of interactions and disorder remains elusive to this day.

Advances in ultracold-atoms experiments [11, 12] have boosted interest in scenarios where disorder and interactions are simultaneously important and new implications emerge from their interplay. An example of recently observed phenomena [13] is many-body localization (MBL) [14, 15], a new experimental and theoretical paradigm where several notions of many-body physics blend coherently [16]. In fact, MBL is part of a broad palette of situations. For example, disorder or interactions alone can produce insulating behavior but, between these limits, how they simultaneously affect conductance is not fully settled [17–23]. In equilibrium, interactions can increase or decrease conductivity in a disordered system [21, 24, 25]. Out of equilibrium, results for quantum rings [26] and quantum transport setups [27] suggest that at fixed disorder strength the current depends non-monotonically on interactions.

To facilitate the description of disordered and interacting systems, it would be useful to have a simple picture. A recent example in this direction was to look at a reduced quantity, the one-body density matrix, to establish a link between MBL, Anderson localization and Fermi-liquid-type features [28, 29]. Another possible reduced description would be in terms of an *independent-particle Hamiltonian*. In a traditional mean-field-intuitive description of disorder vs interactions [22], the low-energy pockets of the rugged potential landscape attract high particle density, but this is opposed by inter-particle repulsion, resulting in a flatter effective potential landscape, i.e. disorder is screened by interactions. It is not unambiguous how to define such potential, and different

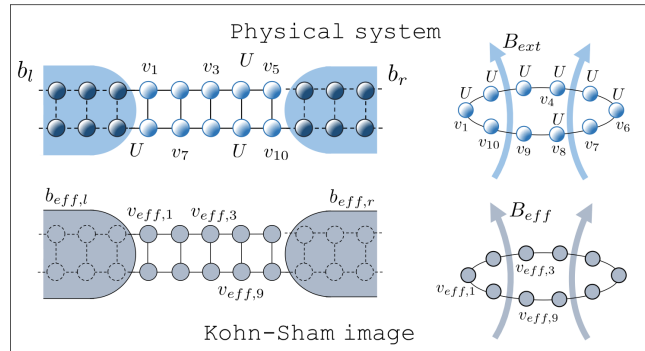


FIG. 1. Many-body and corresponding Kohn-Sham systems for rings and 2D quantum transport setups. The interaction U , the one-body potentials $\{v_i\}$ and KS potentials $\{v_{\text{eff},i}\}$ are shown at representative sites. Due to correlation effects, $b_{\text{eff}} < b$ and $B_{\text{eff}} < B_{\text{ext}}$.

conclusions are reached in the literature [26, 30–34] because of the different definitions of disorder screening and of the theoretical methods used.

Motivated by these arguments, we introduce here a picture of disorder and interactions based on the Kohn-Sham (KS) independent-particle scheme [35] of density functional theory (DFT) [36, 37]. In DFT, the exact density of the interacting system can be obtained from a KS system subjected to an effective potential v_{eff} (Fig. 1). For the density, v_{eff} is the best effective potential in an independent-particle picture. We propose that v_{eff} can be identified as the *independent-particle effective energy landscape in a disordered and interacting system*, which unambiguously defines disorder screening. To assess disorder screening for conductance and currents, we consider out-of-equilibrium systems. In extending DFT to non-equilibrium, we also have to include the notion of an *effective bias* [38–40].

Our main findings are: i) interactions smoothen the effective landscape seen by the electrons (we interpret this as disorder screening); ii) a non-monotonic dependence

of the current on the interaction strength cannot be explained by disorder screening alone; an “effective bias” (corresponding to a screening of the applied bias due to electron correlations) has to be taken into account; iii) The picture from i) and ii) applies to both isolated and open systems and to different dimensionality; iv) our results suggest that DFT can be used as a comprehensive and rigorous diagnostic tool in a variety of situations.

Systems considered. - In this work, we focus on the transition from the weakly to the strongly correlated regime, and consider a single disorder strength. This specific choice is enough to display how the competition of disorder and interaction is captured within a DFT picture. We study quantum rings pierced by magnetic fields and electrically biased quantum-transport setups (Fig. 1). Both situations show the aforementioned current crossover as function of the interaction strength. The rings are solved numerically exactly, while for quantum transport we use the Non-Equilibrium Green’s Function (NEGF) formalism within many-body perturbation theory [41–46] to obtain steady-state currents and densities. The effective potentials and biases were found via a numerical reverse-engineering algorithm [40] within non-equilibrium lattice DFT [47, 48].

Quantum rings. - We study disordered Hubbard rings with $L = 10$ sites, N particles, and spin-compensated, i.e. $N_\uparrow = N_\downarrow = N/2$. Currents are set by a magnetic field threading the rings, via the so-called Peierls substitution [49, 50]. The Hamiltonian is

$$H = -T \sum_{\langle mn \rangle \sigma} e^{i \frac{\phi}{T} x_{mn}} \hat{c}_{m\sigma}^\dagger \hat{c}_{n\sigma} + \sum_{m\sigma} (v_m + \frac{U}{2}) \hat{n}_{m,-\sigma} \hat{n}_{m\sigma}, \quad (1)$$

where $\hat{c}_{m\sigma}^\dagger$ creates an electron with spin projection $\sigma = \pm 1$ at site m , $\hat{n}_{m\sigma} = \hat{c}_{m\sigma}^\dagger \hat{c}_{m\sigma}$. $\langle \dots \rangle$ denotes nearest-neighbor sites. ϕ is the Peierls phase and $x_{mn} = \pm 1$ depending on the direction of the hop from m to n . U is the onsite interaction. We consider onsite energies with box disorder of strength W with $v_m \in [-W/2, W/2]$. In passing, we note that Peierls phases can be realized experimentally in cold atoms by artificial gauge fields [51]. We study currents in rings regimes via exact diagonalization, obtaining the many-body ground-state wavefunction $|\psi(\phi)\rangle$, and the corresponding density matrix $\rho_{mn} = \langle \psi(\phi) | \hat{c}_{n\sigma}^\dagger \hat{c}_{m\sigma} | \psi(\phi) \rangle$. This gives the density at site m as $n_m = 2\rho_{mm}$ and the current as $I = I_{m+1,m} = -4T \text{Im} [e^{i\phi/L} \rho_{m,m+1}]$.

The corresponding effective KS Hamiltonian is

$$h_{KS} = -T \sum_{\langle mn \rangle \sigma} e^{i \frac{\phi^{KS}}{L} x_{mn}} \hat{c}_{m\sigma}^\dagger \hat{c}_{n\sigma} + \sum_{m\sigma} v_m^{KS} \hat{n}_{m\sigma}. \quad (2)$$

The $L + 1$ effective parameters (v_m^{KS}, ϕ^{KS}) are found by solving $h_{KS} \varphi_\nu = \epsilon_\nu \varphi_\nu$ and imposing that the density $n_m = 2 \sum_{\nu=1}^{N/2} |\varphi_\nu(m)|^2$ and bond current $I = -4T \sum_{\nu=1}^{N/2} \text{Im} [e^{i\phi^{KS}/L} \varphi_\nu^*(m+1) \varphi_\nu(m)]$ equal

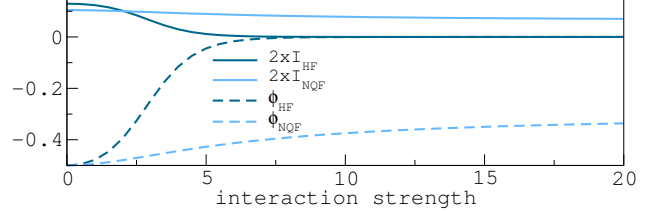


FIG. 2. Current I and KS phase ϕ_{eff} in a 10-site homogeneous ring with density $n = 3/5$ (NQF) and $n = 1$ (HF).

those from the original interacting system. No physical meaning should be *a priori* given to the KS orbitals/eigenvalues; they pertain to an auxiliary system giving the exact density and current but not necessarily other quantities.

The KS potential, referred to as v_{eff} hereafter, is our proposed measure of disorder screening. It can be split into external (disorder) and Hartree-exchange-correlation parts: $v_{\text{eff}} = v + v_{\text{Hxc}}$ (similarly, $\phi_{\text{eff}} \equiv \phi_{\text{KS}} = \phi + \phi_{\text{xc}}$). Thus, in DFT, the screening of disorder by interactions (i.e. when $|v_{\text{eff}}| < |v|$) comes from v_{Hxc} . Both v_{eff} and ϕ_{eff} are obtained by mapping the exact many-body ring system into a DFT-KS one. In lattice models, existence and uniqueness issues for such a DFT-based map can occur [47, 48, 52–55]. Of relevance here, ϕ and $\phi + 2\pi kL$ (k integer) give the same current (uniqueness issue); also, the KS current has an upper bound due to ring periodicity (existence issue). Further, a non-interacting (or described within DFT) homogeneous ring has energy degeneracy for even N_σ (this is lifted by many-body interactions). To circumvent these occurrences, we choose N_σ odd, $-\pi/L < \phi_{\text{eff}} \leq \pi/L$, and consistently choose the region for ϕ_{eff} that smoothly connects to ϕ for small U . Finally, in practice the “maximal current” existence issue is largely mitigated since the target current comes from a physical many-body system.

In the numerical reverse-engineering implementation of the DFT map, ϕ_{eff} and v_{eff} are recursively updated until the many-body and KS system have the same current and density. We use the protocol $[X^{(k+1)} - X^{(k)}][Y_{KS}^{(k)} - Y_{MB}] > 0$, where $(X, Y) \equiv (v_{\text{eff}}, n)$ or (ϕ_{eff}, I) , k is the iteration order, and Y_{MB} is the target many-body value [40].

We consider two electron concentrations: half-filling (HF, $N_\uparrow = 5$), and near quarter-filling (NQF, $N_\uparrow = 3$). Furthermore, we take $T = 1$, i.e. the energy unit. For reference, we start with non-disordered rings, (i.e. $v_i = 0$, which gives $n_i = N/L$ and v_{eff} constant). In Fig. 2, we show HF and NQF currents and corresponding ϕ_{eff} :s as function of the interaction U , for fixed external phase $\phi = -0.5$. Both HF and NQF currents I decrease monotonically with U , but to zero and nonzero values, respectively. This is consistent with Mott insulator behavior at HF and metallic behavior otherwise for $L \rightarrow \infty$ [56].

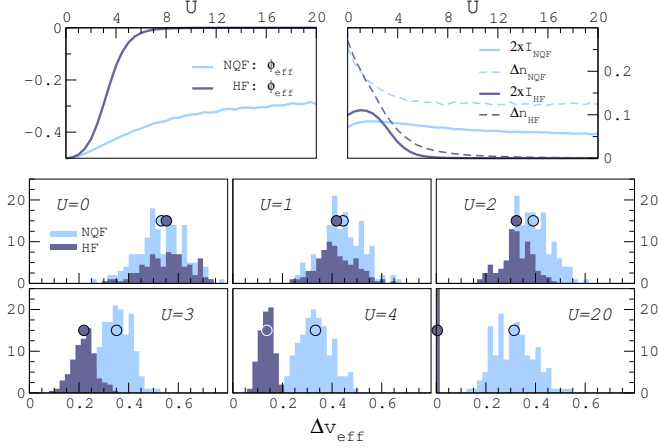


FIG. 3. Disorder vs interactions in 10-site rings near quarter-filling (NQF, $N = 6$) and at half-filling (HF, $N = 10$) for $W = 2$, $\phi = -0.5$. For Δv_{eff} , histograms and disorder averages are shown. For ϕ_{eff} , I , Δn disorder averages are reported.

Finally, in a homogeneous ring the KS orbitals are plane waves and the current is thus determined solely by ϕ_{eff} , showing the importance of the effective phase in our Hamiltonian picture.

We now address the effect of disorder in rings. We use $M = 150$ box-disorder configurations. For a given configuration, the spread ΔX of a quantity X over the $L = 10$ sites is measured by $\Delta X = [L^{-1} \sum_i (\bar{X} - X_i)^2]^{1/2}$, with $\bar{X} = L^{-1} \sum_i X_i$. Results are presented for i) histograms collecting data from each disorder configuration and ii) arithmetic averages over all M configurations. We examine the dependence on the interactions U of the current I , ϕ_{eff} , Δn , and Δv_{eff} . The latter is a measure of disorder screening (in the homogeneous case, $\Delta v_{\text{eff}} = 0$ for all U). With disorder ($W = 2$), for both NQF and HF the current I is hindered by disorder at low U and by interactions at large U , with a maximum in between (Fig. 3). As for $W = 0$ (Fig. 2), for HF I vanishes at very large U . The non-monotonic behavior of I results from competing disorder and interactions [21, 26, 27]. Conversely, the density spread Δn decreases monotonically as a function of U at both NQF and HF, i.e. interactions favor a more homogeneous density. For NQF, Δn seems to tend to a finite value for large U , while for the HF case, $\Delta n \rightarrow 0$, i.e. a fully homogeneous density. In the KS system, Δv_{eff} also decreases monotonically as function of U , tending to a finite value for NQF and to zero for HF. This means that the *exact* v_{eff} for a strongly correlated system is smoother than for a weakly correlated system, and similarly for the density. Thus, we cannot simply look at the spread of the density to predict the current through the system: Including the effective phase is crucial.

The competition of disorder and interactions thus translates into a competition of a decreasing effective potential spread (favoring the current) and a decreasing ef-

fective phase (reducing the current). Mean-field [26] or DFT-LDA treatments [57] fail to explain the current drop since they only take the effective potential into account: With an effective potential and no effective phase, the current can only increase with interactions. This ends our discussion on exact treatments of quantum rings.

Open systems. - We study short clusters connected to semi-infinite leads, with Hamiltonian $\hat{H} = \hat{H}_C + \hat{H}_l + \hat{H}_{Cl}$, where C , l , and Cl label the cluster, leads, and cluster-leads coupling parts, respectively. With the same notation as for rings,

$$\hat{H}_C = -T \sum_{\langle mn \rangle \in C, \sigma} \hat{c}_{m\sigma}^\dagger \hat{c}_{n\sigma} + \sum_{m\sigma} v_m \hat{n}_{m\sigma} + U \sum_i \hat{n}_{m\uparrow} \hat{n}_{m\downarrow}. \quad (3)$$

Also in this case, we have box disorder, $v_m \in [-W/2, W/2]$. Depending on the cluster dimensionality, the leads are either 1D (chain) or 2D (strip) semi-infinite tight-binding structures. The latter case is shown in Fig. 1. The lead Hamiltonian is $\hat{H}_l = \sum_{\alpha} \hat{H}_{\alpha}$, and $\alpha = r(l)$ refers to the right (left) contact: $\hat{H}_{\alpha} = -T \sum_{\langle mn \rangle \in \alpha, \sigma} T_{mn} \hat{c}_{m\sigma}^\dagger \hat{c}_{n\sigma} + b_{\alpha}(t) \hat{N}_{\alpha}$. Here, $b_{\alpha}(t)$ is the (site-independent) bias in lead α , and $\hat{N}_{\alpha} = \sum_{m \in \alpha, \sigma} \hat{n}_{m\sigma}$ the number operator in lead α . Finally, the lead-cluster coupling \hat{H}_{Cl} connects the edges of the central region to the leads (Fig. 1) with tunneling parameter $-T$. In the following, $T = 1$, the energy unit. We focus on the steady-state scenario with $b_r(t) = 0$, and $b_l \equiv b_l(t \rightarrow \infty) = 1$, beyond the linear regime. Our 1D and 2D clusters have $L = 10$ sites, but are large enough to illustrate the relevant physics and the scope of a DFT perspective. Also, we put $n_{\uparrow} = n_{\downarrow} = n$ (non-magnetic case) and the temperature to zero.

Steady-State Green's functions. - Both our many-body (MB) and KS treatments are based on NEGF in its steady-state formalism. Thus we keep our presentation general, and later specialize to MB or KS. To describe the steady-state regime, we use retarded $\mathbf{G}^R(\omega)$ and lesser $\mathbf{G}^<(\omega)$ Green's functions:

$$\mathbf{G}^R(\omega) = [\omega \mathbf{1} - \mathbf{T} - \mathbf{v} - \mathbf{\Sigma}^R(\omega)]^{-1}, \quad (4)$$

$$\mathbf{G}^<(\omega) = \mathbf{G}^R(\omega) \mathbf{\Sigma}^<(\omega) \mathbf{G}^A(\omega). \quad (5)$$

Here, boldface quantities denote $L \times L$ matrices in site indices of the cluster region, $\mathbf{G}^A = (\mathbf{G}^R)^\dagger$, $(\mathbf{T})_{mn} = T_{mn}$ is the kinetic term of Eq. (3), and \mathbf{v} is not specified yet. The self-energy $\mathbf{\Sigma}$ contains many-body (MB) and embedding (emb) parts: $\mathbf{\Sigma}^{R/<} = \mathbf{\Sigma}_{\text{MB}}^{R/<} + \mathbf{\Sigma}_{\text{emb}}^{R/<}$. All correlation effects are contained in the many-body self-energy $\mathbf{\Sigma}_{\text{MB}}^{R/<}$, whilst the embedding term accounts in an exact way for the left (l) and right (r) leads [58]: $\mathbf{\Sigma}_{\text{emb}}^{R/<} = \sum_{\alpha=l,r} \mathbf{\Sigma}_{\alpha}^{R/<}$. More explicitly, $\mathbf{\Sigma}_{\alpha}^{<}(\omega) = i f_{\alpha}(\omega) \mathbf{\Gamma}^{\alpha}(\omega)$, where $\mathbf{\Gamma}^{\alpha} = -2 \text{Im} [\mathbf{\Sigma}_{\alpha}^R]$ and $f_{\alpha}(\omega) = \theta(-\omega + \mu + b_{\alpha})$. Thus, information of the actual structure of the leads, the bias b_{α} and the chemical potential μ enters via f_{α}

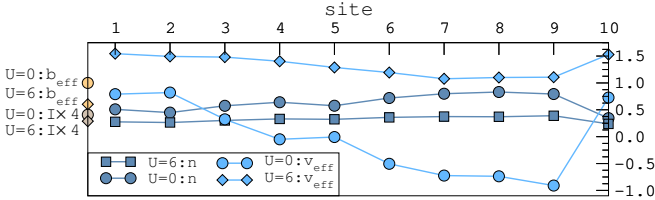


FIG. 4. Density n , effective potential v_{eff} , effective bias b_{eff} and current I (multiplied by 4 for convenience) for a specific disordered wire with $W = 2$ and bias $b = 1$ for $U = 0$ and 6.

and Σ_{emb}^R . Explicit expressions of Σ_{emb}^R exist for 1D and 2D semi-infinite leads [59], since they are determined the uncontacted-lead case.

For our system, the steady-state particle density and current are spin-independent. In each spin channel [60], with I_l the left lead current, and the spin-labels omitted,

$$n_k = \int_{-\infty}^{\infty} \frac{d\omega}{2\pi i} G_{kk}^<(\omega), \quad (6)$$

$$I_l = \int_{-\infty}^{\infty} \frac{d\omega}{2\pi i} \text{Tr} [\Gamma^l(\omega) (G^<(\omega) - 2\pi i f_l(\omega) \mathbf{A}(\omega))]. \quad (7)$$

where $2\pi\mathbf{A} = i(G^R - G^A)$. MB and KS cases are both described by Eqs. (4-7). We now specialize the discussion.

MB) Here $(\mathbf{v})_{ij} = \delta_{ij} v_i$ are the disordered onsite energies, b_α is the applied bias, and $\Sigma_{\text{MB}}^{R/<} = \Sigma_{\text{MB}}^{R/<}[G^R, G^<]$. For Σ_{MB} we use the 2nd Born approximation [27, 58, 61, 62], keeping all diagrams up to second order. The equations are solved self-consistently, with the convergence improved with the Pulay scheme [62, 63]. In this way, general conservation laws [64, 65], and in particular the continuity equation [66], are fulfilled, i.e. if I_α is the current from lead α , then $I_l = -I_r = I$.

KS) Here $\Sigma_{\text{MB}}^{R/<} = 0$. Further, $(\mathbf{v})_{ij} \equiv \delta_{ij} v_{i,\text{eff}}$ and $b_\alpha \equiv b_{\text{eff},\alpha}$ are found iteratively to make the KS and MB density and current the same [40]. The embedding self-energies in the KS and MB systems differ only by the bias (effective in KS, applied in MB). We restrict $b_{\text{eff},r} = 0$ and define $b_{\text{eff}} = b_{\text{eff},l}$. The KS independent-particle scheme permits to write $I = \int_{\mu}^{\mu+b_{\text{eff}}} \frac{d\omega}{2\pi} T_{\text{KS}}(\omega)$, with $T_{\text{KS}} = \text{Tr} [\Gamma^l G^R \Gamma^r G^A]$ the KS transmission function. Although recast in a Landauer-Büttiker form, the KS current still equals the true current.

Open systems: Results. - In the following, we put $\mu_\alpha = 0$ (half-filled leads). To address the behavior of v_{eff} in quantum transport setups, we find it useful to start with one disorder configuration and two interaction values for a biased 10-site one-dimensional chain (Fig. 4). At $U = 0$, the density n_k is non-uniform, since $v_{\text{eff}} = v$ and $b_{\text{eff}} = b$. For $U = 6$, both n_k and v_{eff} (now incorporating correlations) become smoother: interactions thus provide a smoother energy landscape also for open systems. However, $I_{U=6} < I_{U=0}$, even if the effective energy

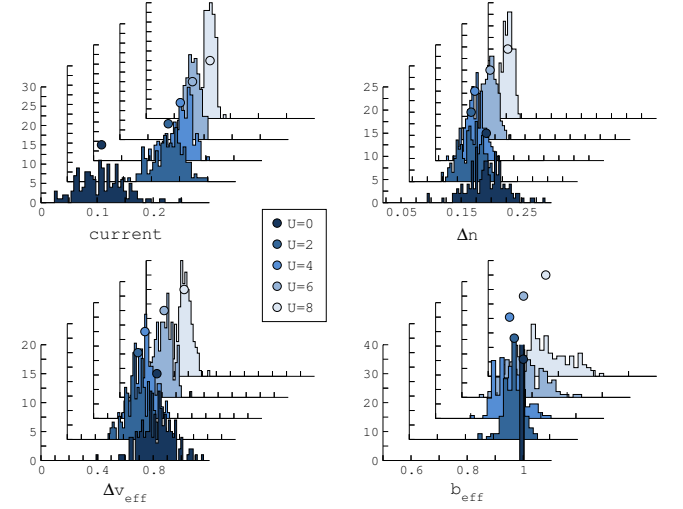


FIG. 5. Histograms of Δn , Δv_{eff} , I and b_{eff} and their arithmetical averages (dots) for the 2D system of Fig. 1 with $W = 3$ and bias $b = 1$. The corresponding statistical errors $\sigma_x = \frac{\bar{x}}{\sqrt{M}}$ are comparable or smaller than the dot sizes, and thus not shown. Results for the 1D open system exhibit similar trends.

landscape is smoother. This is due to b_{eff} , that at $U = 6$ is much smaller than b [39, 40, 67].

To corroborate this analysis, we consider the 2D open system of Fig. 1. Results from 150 disorder configurations for Δn , Δv_{eff} (defined as for rings), I , and b_{eff} are shown in Fig. 5 [68]. The current through the system is a non-monotonic function of U , while Δn , Δv_{eff} decrease monotonically. At low U , b_{eff} almost equals b , and I increases since Δv_{eff} decreases. At larger U , however, the drop in b_{eff} grows, and I is smaller. This is why I shows a crossover. Thus, the competition between disorder and interactions in open systems transfers to a competition between the smoothness of the energy landscape favoring current flow and screening of the effective bias hindering such flow. Finally, we mention that the corresponding 1D linear chain exhibit similar trends (not shown).

Conclusions. - We introduced an exact independent-particle characterization of coexisting disorder and interaction effects, based on DFT. Its scope as a diagnostic for disorder screening was shown for open-sample geometries and small quantum rings. The many-body treatment of the quantum rings was exact, to unambiguously characterize disorder screening. For open systems we used NEGF, with biased reservoirs treated exactly and electronic correlations via the 2nd Born approximation, which is quite accurate at low interaction strengths [61, 69, 70]. The same results were found using the T-matrix approximation [61, 71–73] (not shown) for selected configurations. The general picture that emerges from our study is that effective-potential and density distributions cannot be taken alone as a measure of conductance, since their spread is always reduced by interactions, even when the current is non-monotonic. One

must also include the effective bias / phase.

To conclude, within our Hamiltonian independent-particle picture, strong correlation effects are behind the appearance of the effective potential and bias, and this is the essence of disorder screening. As possible extensions of our approach, we mention applications to real materials and the generalization to finite temperatures [74] to describe, for example, the many-body localized regime. These are deferred to future work.

We acknowledge Fabian Heidrich-Meisner for useful discussions. D.K. would like to thank the Academy of Finland for support under project no. 267839.

* Corresponding author:daniel.l.e.karlsson@jyu.fi

- [1] M. Imada, A. Fujimori, and Y. Tokura, *Rev. Mod. Phys.* **70**, 1039 (1998).
- [2] E. Wigner, *Phys. Rev.* **46**, 1002 (1934).
- [3] J. H. de Boer and E. J. W. Verwey, *Proc. Phys. Soc.* **49**, 59 (1937).
- [4] N. F. Mott and R. Peierls, *Proc. Phys. Soc.* **49**, 72 (1937).
- [5] N. F. Mott, *Proc. Phys. Soc. Sect. A* **62**, 416 (1949).
- [6] J. Korringa, *J. Phys. Chem. Solids* **7**, 252 (1958).
- [7] P. W. Anderson, *Phys. Rev.* **109**, 1492 (1958).
- [8] J. T. Edwards and D. J. Thouless, *J. Phys. C Solid State Phys.* **5**, 807 (1972).
- [9] F. Gebhard, *The Mott Metal-Insulator Transition*, Springer Tracts in Modern Physics, Vol. 137 (Springer Berlin Heidelberg, Berlin, Heidelberg, 2000).
- [10] E. Abrahams, P. W. Anderson, D. C. Licciardello, and T. V. Ramakrishnan, *Phys. Rev. Lett.* **42**, 673 (1979).
- [11] M. Lewenstein, A. Sanpera, V. Ahufinger, B. Damski, A. Sen(De), and U. Sen, *Adv. Phys.* **56**, 243 (2007).
- [12] I. Bloch, J. Dalibard, and S. Nascimbène, *Nat. Phys.* **8**, 267 (2012).
- [13] J.-y. Choi, S. Hild, J. Zeiher, P. Schauss, A. Rubio-Abadal, T. Yefsah, V. Khemani, D. A. Huse, I. Bloch, and C. Gross, *Science* **352**, 1547 (2016).
- [14] I. V. Gornyi, A. D. Mirlin, and D. G. Polyakov, *Phys. Rev. Lett.* **95**, 206603 (2005).
- [15] D. Basko, I. Aleiner, and B. Altshuler, *Ann. Phys. (N. Y.)* **321**, 1126 (2006).
- [16] R. Nandkishore and D. A. Huse, *Annu. Rev. Condens. Matter Phys.* **6**, 15 (2015).
- [17] B. Kramer and A. MacKinnon, *Reports Prog. Phys.* **56**, 1469 (1993).
- [18] S. V. Kravchenko, G. V. Kravchenko, J. E. Furneaux, V. M. Pudalov, and M. D'Iorio, *Phys. Rev. B* **50**, 8039 (1994).
- [19] S. V. Kravchenko, W. E. Mason, G. E. Bowker, J. E. Furneaux, V. M. Pudalov, and M. D'Iorio, *Phys. Rev. B* **51**, 7038 (1995).
- [20] S. V. Kravchenko, D. Simonian, M. P. Sarachik, W. Mason, and J. E. Furneaux, *Phys. Rev. Lett.* **77**, 4938 (1996).
- [21] T. Vojta, F. Epperlein, and M. Schreiber, *Phys. Rev. Lett.* **81**, 4212 (1998).
- [22] R. T. Scalettar, in *AIP Conf. Proc.*, Vol. 918 (AIP, 2007) pp. 111–202.
- [23] E. Lahoud, O. N. Meetei, K. B. Chaska, A. Kanigel, and

- N. Trivedi, *Phys. Rev. Lett.* **112**, 206402 (2014).
- [24] P. J. H. Denteneer, R. T. Scalettar, and N. Trivedi, *Phys. Rev. Lett.* **83**, 4610 (1999).
- [25] E. Abrahams, S. V. Kravchenko, and M. P. Sarachik, *Rev. Mod. Phys.* **73**, 251 (2001).
- [26] A. Farhoodfar, R. J. Gooding, and W. A. Atkinson, *Phys. Rev. B* **84**, 205125 (2011).
- [27] D. Karlsson and C. Verdozzi, *Phys. Rev. B* **90**, 201109 (2014).
- [28] S. Bera, H. Schomerus, F. Heidrich-Meisner, and J. H. Bardarson, *Phys. Rev. Lett.* **115**, 046603 (2015).
- [29] S. Bera, T. Martynec, H. Schomerus, F. Heidrich-Meisner, and J. H. Bardarson, *Ann. Phys.* **529**, 1600356 (2017).
- [30] D. Tanasković, V. Dobrosavljević, E. Abrahams, and G. Kotliar, *Phys. Rev. Lett.* **91**, 066603 (2003).
- [31] P. Henseler, J. Kroha, and B. Shapiro, *Phys. Rev. B* **77**, 075101 (2008).
- [32] P. Henseler, J. Kroha, and B. Shapiro, *Phys. Rev. B* **78**, 235116 (2008).
- [33] Y. Song, R. Wortis, and W. A. Atkinson, *Phys. Rev. B* **77**, 054202 (2008).
- [34] M. E. Pezzoli and F. Becca, *Phys. Rev. B* **81**, 075106 (2010).
- [35] W. Kohn and L. J. Sham, *Phys. Rev.* **140**, A1133 (1965).
- [36] P. Hohenberg and W. Kohn, *Phys. Rev.* **136**, B864 (1964).
- [37] E. Runge and E. K. U. Gross, *Phys. Rev. Lett.* **52**, 997 (1984).
- [38] P. Schmitteckert, M. Dzierzawa, and P. Schwab, *Phys. Chem. Chem. Phys.* **15**, 5477 (2013).
- [39] G. Stefanucci and S. Kurth, *Nano Lett.* **15**, 8020 (2015).
- [40] D. Karlsson and C. Verdozzi, *J. Phys. Conf. Ser.* **696**, 012018 (2016).
- [41] L. P. Kadanoff and G. Baym, *Quantum Statistical Mechanics* (Benjamin, New York, 1962).
- [42] L. Keldysh, *Sov. Phys. JETP* **20**, 1018 (1965).
- [43] H. Haug and A. Jauho, *Quantum Kinetics in Transport and Optics of Semiconductors*, Solid-State Sciences, Vol. 123 (Springer Berlin Heidelberg, Berlin, Heidelberg, 2008).
- [44] G. Stefanucci and R. van Leeuwen, *Nonequilibrium Many-Body Theory Quantum Systems: A Modern Introduction* (Cambridge University Press, Cambridge, 2013).
- [45] K. Balzer and M. Bonitz, *Nonequilibrium Green's Functions Approach to Inhomogeneous Systems*, Lecture Notes in Physics, Vol. 867 (Springer Berlin Heidelberg, Berlin, Heidelberg, 2013).
- [46] M. Hopjan and C. Verdozzi, in *First Principles Approaches to Spectroscopic Properties of Complex Materials*, Vol. 11 (Springer Berlin Heidelberg, 2014) pp. 347–384.
- [47] C. Verdozzi, *Phys. Rev. Lett.* **101**, 166401 (2008).
- [48] M. Farzanehpour and I. V. Tokatly, *Phys. Rev. B* **86**, 125130 (2012).
- [49] R. E. Peierls, *Z. Phys.* **80**, 763 (1933).
- [50] D. R. Hofstadter, *Phys. Rev. B* **14**, 2239 (1976).
- [51] K. Jiménez-García, L. J. LeBlanc, R. A. Williams, M. C. Beeler, A. R. Perry, and I. B. Spielman, *Phys. Rev. Lett.* **108**, 225303 (2012).
- [52] R. Baer, *J. Chem. Phys.* **128**, 044103 (2008).
- [53] Y. Li and C. A. Ullrich, *J. Chem. Phys.* **129**, 044105 (2008).
- [54] G. Stefanucci, E. Perfetto, and M. Cini, *Phys. Rev. B*

81, 115446 (2010).

[55] S. Kurth and G. Stefanucci, *Chem. Phys.* **391**, 164 (2011).

[56] E. H. Lieb and F. Y. Wu, *Phys. Rev. Lett.* **20**, 1445 (1968).

[57] V. Vettchinkina, A. Kartsev, D. Karlsson, and C. Verdozzi, *Phys. Rev. B* **87**, 115117 (2013).

[58] P. Myöhänen, A. Stan, G. Stefanucci, and R. van Leeuwen, *EPL (Europhysics Lett.)* **84**, 67001 (2008).

[59] P. Myöhänen, R. Tuovinen, T. Korhonen, G. Stefanucci, and R. van Leeuwen, *Phys. Rev. B* **85**, 075105 (2012).

[60] Y. Meir and N. S. Wingreen, *Phys. Rev. Lett.* **68**, 2512 (1992).

[61] M. Puig von Friesen, C. Verdozzi, and C.-O. Almbladh, *Phys. Rev. Lett.* **103**, 176404 (2009).

[62] K. S. Thygesen and A. Rubio, *Phys. Rev. B* **77**, 115333 (2008).

[63] P. Pulay, *Chem. Phys. Lett.* **73**, 393 (1980).

[64] G. Baym and L. P. Kadanoff, *Phys. Rev.* **124**, 287 (1961).

[65] G. Baym, *Phys. Rev.* **127**, 1391 (1962).

[66] D. Karlsson and R. van Leeuwen, *Phys. Rev. B* **94**, 125124 (2016).

[67] G. Stefanucci and C.-O. Almbladh, *Phys. Rev. B* **69**, 195318 (2004).

[68] We do not include results from a small fraction of calculations ($\sim 1\%$), which did not converge.

[69] A.-M. Uimonen, E. Khosravi, A. Stan, G. Stefanucci, S. Kurth, R. van Leeuwen, and E. K. U. Gross, *Phys. Rev. B* **84**, 115103 (2011).

[70] S. Hermanns, N. Schlünzen, and M. Bonitz, *Phys. Rev. B* **90**, 125111 (2014).

[71] V. Galitskii, *Sov. Phys. JETP* **34**, 104 (1958).

[72] M. Puig von Friesen, C. Verdozzi, and C.-O. Almbladh, *EPL (Europhysics Lett.)* **95**, 27005 (2011).

[73] N. Schlünzen, S. Hermanns, M. Bonitz, and C. Verdozzi, *Phys. Rev. B* **93**, 035107 (2016).

[74] N. D. Mermin, *Phys. Rev.* **137**, A1441 (1965).